Modeling and forecasting relative humidity using multilayer perceptron, radial basis function, and linear regression approaches

Iman Kadir[1*] , Abdellah Ben Yahia[1] , Abdelaziz Abdallaoui[1] , Abdellah El Hmaidi[2]

[1] Department of Chemistry, Laboratory of Analytical Chemistry and Electrochemistry, Processes and Environment, Moulay Ismail University, Faculty of Sciences, Meknes, Morocco
[2] Department of Geology, Laboratory of Water Sciences and Environmental Engineering, Moulay Ismail University, Faculty of Sciences, Meknes, Morocco
* Corresponding author's e-mail: iman.kadir@edu.umi.ac.ma

ABSTRACT

Forecasting relative humidity is a critical for addressing the challenges of climate change. It facilitates comprehension of climatic mechanisms and the anticipation of extreme weather events, while also contributing to strengthening societal resilience and protection. Indeed elevated levels of humidity have been demonstrated to exacerbate heat waves, leading to a marked increase in both the perceived temperature and the associated health risks. Conversely, low humidity promotes conditions conducive to droughts and wildfires. Moreover, relative humidity plays a key role in the water cycle, influencing precipitation, evaporation, and cloud formation. Understanding these mechanisms is essential for anticipating floods, droughts, and water shortages. In this study, mathematical models were developed to predict relative humidity in the Fez, Morocco, using multilayer perceptron (MLP) neural networks, radial basis function (RBF) neural networks, and multiple linear regression (MLR). The dataset used in this study includes daily values of eight meteorological parameters, including temperature at 2m, shortwave radiation, diffuse shortwave radiation, precipitation total, evapotranspiration, vapor pressure deficit and wind speed and relative humidity as the output. The data spans 38 years, from January 1985 to December 2022, and includes 13879 observation days. To evaluate the predictive performance of these models, we analyzed their architectures, learning algorithms, correlation coefficients, and mean squared errors. The results indicate that the MLP model attains the highest predictive accuracy, with a correlation coefficient of 0.9809 and a mean squared error MSE of 0.0099, outperforming the RBF model (correlation of 0.9603) and the MLR model (correlation of 0.9023), the best performing model used a Tansig activation function in the hidden layer, a Purelin function in the output layer and the Levenberg-Marquardt learning algorithm with a MLP configuration [7-15-1]. The findings of this study offer a valuable contribution to the field of water resource management in the region. They demonstrate the efficacy of artificial neural network models in enhancing moisture forecasting, thereby providing a solid foundation for future research in climate modelling.

Keywords: modeling, MLP, RBF, MLR, climate change, correlation coefficient, mean square errors, relative humidity, Fez.

INTRODUCTION

Relative humidity (RH) is one of the most important hydroclimatic factors directly affecting the environment. In the current climate, environmental disturbances, particularly global climate change, represent a major concern in the climatological research sector. In view of the global challenges we face, there is an imperative to enhance our compression and predict RH, given its significant impact on human health, ecological systems and the increasing frequency of extreme weather events. RH is defined as the ratio between the maximum quantity of water vapor in the atmosphere and the amount of water vapor that the air can contain at a certain temperature [1]. The temperature of the air can affect its relative humidity. An increase in air temperature leads to an increase in the amount of water vapor in the

air, thereby enhancing the humidity level. Low humidity has been linked to the development of respiratory viruses such as influenza and coronaviruses [2–5]. Furthermore, excessive humidity can reduce the body's ability to regulate its temperature and promote the growth of bacteria and fungi, which can have a negative impact on respiratory health.

In view of the critical role of relative humidity in environmental processes, a number of studies have concentrated on enhancing its predictive accuracy. Forecasting relative humidity has become increasingly important due to its significant impact on ecological systems, human health, and climate change. A variety of machine learning algorithms have been used, with varying degrees of success in predicting RH. Recent advancements in forecasting techniques have been driven by the need to better understand and predict climate-related phenomena in the face of these challenges [6, 7].

Machine learning models, in particular artificial neural networks (ANNs), have demonstrated considerable potential in predicting RH. However, existing models frequently encounter difficulties accounting for regional climatic variations. In this regard, multilayer perceptron (MLP) and radial basis function (RBF) networks have demonstrated superior performance in predicting environmental variables, especially when handling non-linear relationships in the data. Research has demonstrated that MLP and RBF networks provide enhanced flexibility in modelling environmental parameters in comparison to traditional methods [8, 9].

The present study uniquely focuses on the Fez region in Morocco, where there is limited research on predicting relative humidity using MLP and RBF networks. The objective of this study is to enhance the accuracy of RH predictions by integrating regional climatic conditions and local meteorological data. This approach aims to address the challenges associated with the application of machine learning models in specific geographic contexts. The selection of these models is predicated on their demonstrated capacity to manage the complex, non-linear relationships between meteorological parameters and RH. A recent study evaluated several machines learning algorithms, including gradient boosting tree (GBT), random forest (RF), linear regression (LR), and two ANN architectures (MLP and RBF). The study concluded that the MLP-NN model performed best for daily temperature and humidity predictions [10]. This supports the efficacy of MLP and RBF networks in modelling temperature and humidity dynamics, further justifying their use in this study. For instance, Ben Yahia *et al.* [11] found that RBF networks performed better than exponential regression in predicting humidity variations, while Khatibi *et al.* [12] showed that ANN outperformed GEP when incorporating both current and historical data in the presence of noisy data.

The objective of this study is to develop a precise mathematical model for predicting relative humidity based on different meteorological factors, specifically tailored to the Fez region. This will be comparing the performance of MLP and RBF networks, which is expected to provide valuable insights into the modelling of RH in regions with unique climatic conditions. The findings of this study are expected to contribute to the development of robust and region-specific predictive models for RH, aiding in environmental monitoring, public health applications, and climate-related studies. The cost/loss function employed in this case to measure the performance of the model on the entire dataset is the mean squared error (MSE). This is the loss function that evaluates the errors between the model's predictions and the actual values and the correlation coefficient (R).

MATERIALS AND METHODS

Materials

Database

In this study, we used a daily database of 13879 days and eight meteorological variables for the city of Fez (Fig. 1), recorded between January 1985 and December 2022. The database included the following:

- Seven independent explanatory variables: temperature at 2 m, shortwave radiation, diffuse shortwave radiation, precipitation total, evapotranspiration, vapor pressure deficit and wind speed.
- The dependent variable to be predicted is the relative humidity.

Table 1 presents a meteorological variable, with their respective abbreviations and units of measurement.

Figure 1. Geographical location of the study area

Table 1. The meteorological parameters used in this study and their respective designations

Meteorological variables	Designation	Unit	Types de variable
Temperature	T	°C	Independent variables
Shortwave radiation	SR	W/m²	
Diffuse shortwave radiation	DSR	W/m²	
Precipitation total	PT	mm	
Evapotranspiration	E_v	mm	
Vapor pressure deficit	VPD	hPa	
Wind speed	WS	Km/h	
Relative humidity	RH	%	Dependent variable

Database normalization

The database has undergone a pre-processing stage that includes appropriate normalization of its data, taking into consideration the amplitude of the values accepted by the network. The database has been normalized to a range between -1 and 1 for its maximum and minimum values, as detailed in the following normalization equation [13].

$$\overline{X_\iota} = \frac{2(X_i - X_{i(min)})}{(X_{i(max)} - X_{i(min)})} - 1 \qquad (1)$$

where: $\overline{X_\iota}$ – normalized values of variable i; X_i – raw, non-normalized values of variable i; $X_{i(min)}$ – minimum values of variable i; and $X_{i(max)}$ – maximum values of variable i.

Methods

Multiple linear regression

MLR is a statistical tool used to predict the values of a dependent variable based on independent variables. The goal is to identify the most accurate model for predicting the dependent value to minimize error. The equation for the MLR model is represented as follows [14].

$$Y = a_0 + a_1 X_1 + a_2 X_2 + \cdots + + a_n X_n + \varepsilon_i, \qquad (2)$$

where: Y – dependent variable; X_1, X_2, ..., X_n – independent variables; a_0 – estimated intercept; a_1; a_2; ...; a_n – slopes (partial regression coefficients); n – number of explanatory variables; and ε_i – a residual.

Artificial neural network design

An artificial neural network (ANN) is a methodology used in the field of artificial intelligence. It is defined by a structured set of units (neurons) that operate in parallel and in a distributed manner to achieve the optimal outcome according to a defined set of objectives. The network is capable of receiving inputs and producing an output result [15, 16].

An artificial neuron is capable of receiving a variable number of inputs, with each input being associated with a weight that represents the strength of the connection. Each processor generates a distinct output, which then serves as an input to feed a variable number of neurons [17].

MLP artificial neural networks

Neural networks are categorized into distinct classification, each with its specific applications and utilization. For the purposes of this study, the multilayer perceptron has been selected as the network model. The rationale behind this selection is twofold: firstly, its rapid and straightforward construction for databases with limited variables and secondly, its efficacy in addressing the research questions at hand [18] (Fig. 2).

A multilayer perceptron consists of neurons distributed over several layers, with information flowing exclusively from the input layer to the output layer. The input layer contains neurons in accordance with the number of dimensions present in the input space, while the output layer consists of a single neuron that represents the predicted value. Additionally, the network contains one or more hidden layers located between the input and output layers, with the number of neurons in each layer varying [19].

Artificial neural networks of the RBF type

The radial basis function network is a type of supervised artificial neural network. It consists of three layers: an input layer, a single hidden layer with neurons activated by the gaussian activation function [19, 20] and an output layer with neurons activated by the linear activation function (Fig. 3).

The information begins at the input layer, then moves to the hidden layer, and finally ends at the output layer. A principal feature of RBF networks pertains to the training process employed to adjust the weights of the two layers of neurons [22].

The hidden layer consists of k nodes, with each node applying a non-linear transformation to the input variables. Each node, designed by 'j'

possesses a center, denoted by C_j, which is a vector with dimensions equal to the number of inputs. Upon reception of a new input vector $X = [X_1, X_2,..., X_n]$, the Euclidean distance between the input vector and the node center is calculated using the following formula:

$$v_j(X) = \|C_j - X\| = \sqrt{\sum_{i=1}^{n}(X_i - C_{ji})^2} \quad (3)$$

where: v_j – the norm of the Euclidean distance between the input vector and the node center; C_j – the center associated with neuron, j – a vector of dimension equal to the number of inputs.

$X = [x_1, x_2, \ldots, x_n]$: input vector.

The output of the hidden layer nodes is determined by a non-linear activation function, specifically a Gaussian function:

$$f(v) = exp\left(-\frac{v^2}{\sigma^2}\right) \quad (4)$$

where: σ – standard deviation of the activation function.

In this context, σ represents the standard deviation of the activation function. As a general guideline, the following approach is recommended:

$$\sigma_j = \frac{d_j}{\sqrt{2M}} \quad (5)$$

where: d_j – the maximum distance between center j and the other remaining centers; M – the total number of centers in the hidden layer.

The connections between the hidden layer and the output layer are assigned a set of synaptic weights W_j, where $j = 1, 2..., k$. The nodes in the output layer essentially perform a summation
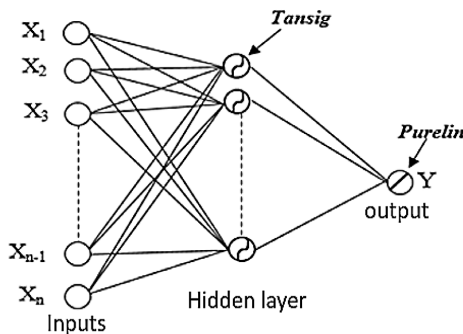

Figure 2. Example of an MLP neural network architecture with a Tansig activation function in the hidden layer
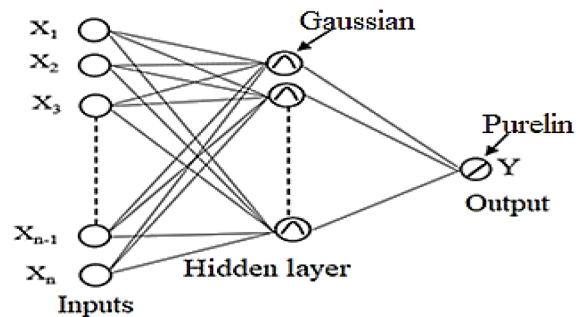

Figure 3. Example of an RBF neural network architecture with a gaussian activation function in the hidden layer

function to produce the final output of the network. The output of the output layer is provided as follows:

$$Y = L(\textstyle\sum_{j=1}^{k} W_j Z_j + b_j) \qquad (6)$$

where: L(n) = n linear function; w_j, j = 1,2...,
k – set of synaptic weights; b_j – the bias.

The connections between the hidden layer and the output layer are determined based on the target vector, Y = [Y_1, Y_2,..., Y_n] [21]:

$$W = inv\ (Z^T Z)\ Z^T Y^T \qquad (7)$$

where: *inv* – the inverse.

Statistical performance criteria

In this research, two criteria were employed to assess the performance of the model: the correlation coefficient (R) [13] and the mean squared error (MSE) [23]. These criteria are utilized to compare the accuracy of various models. To conduct these calculations, two sets of predictions and observations of relative humidity are required. The following equations are employed to derive these values:

$$R = \sqrt{1 - \frac{\sum_{j=1}^{N}(Y_{Pj} - Y_{Oj})}{\sum_{j=1}^{N}(Y_{Oj} - Y_m)}} \qquad (8)$$

where: Y_{Pj} and Y_{oj} – predicted and observed values correspondingly; N – number of observations; Y_m – mean of the observed values.

$$MSE = \frac{1}{N}\sum_{j=1}^{N}(Y_{Pj} - Y_{Oj})^2 \qquad (9)$$

RESULTS AND DISCUSSION

Multiple linear regression (MLR)

A multiple linear regression analysis was conducted using XLSTAT software to identify an appropriate linear model for predicting relative humidity, based on the independent variables. The resulting equation for this model is as follows:

RH (%) = 63.236 + 1.110 × T – 7.439 × 10^{-3} × SR – 8.023 × 10^{-2} × DSR + 0.706 × PT + 52.464 × E_v – 1.844× VPD + 5.554 × 10^{-2} × WS

The coefficient obtained by the MLR model is R = 0.902, and the mean square error is MSE = 58.08. The relatively low value of R and the high value of MSE, in comparison with those of MLP-type neural models, confirm that there is no linear correlation between RH and the other meteorological parameters. Furthermore, they demonstrate the limitations of the MLR model in terms of its capacity for modeling.

The analysis of the model predictor variables reveals that all variables, including temperature, solar radiation, precipitation, evapotranspiration, vapor pressure deficit, and wind speed are statistically significant, with very low p-values (< 0.0001 for the majority), indicating their substantial influence in predicting relative humidity. While certain variables, including direct and diffuse solar radiation, are strongly correlated, they provide distinct information and justify their inclusion in the model. No variable was considered to be redundant or statistically insignificant. Nevertheless, it is acknowledged that techniques such as principal component analysis (PCA) could be employed in future studies to address any possible multicollinearity.

In order to predict this parameter with greater accurately, mathematical models have been developed based on artificial neural networks.

Artificial neural networks

MLP neural network

In this study, we employed supervised neural networks of the MLP type, as they are well-suited to the predictive modeling tasks of the study. It is acknowledged that these networks are capable of addressing non-linear problems in addition to prediction.

To identify the optimal configuration for the MLP network, a series of experiments where conducted. These experiments studied the effect of data distribution, number of hidden layers, number of neurons in each hidden layer, activation function pairs, and learning algorithms [23].

Initially, the database is divided into three distinct sets: a training set, a test set and a validation set, with respective proportions of 70%, 15% and 15% respectively. This distribution of data is a common practice in the relevant literature, with the aim of avoiding overlearning and ensuring robust evaluation of the models [24].

The following Table 2 illustrates the values of the performance indicators R and MSE as a function of the number of hidden layers. It was observed that an increase in the number of hidden

Table 2. Values of R and MSE as a function of the number of hidden layers

Number of hidden layers	R	MSE x 10^{+2}
1	0.9783	1.14
2	0.9277	3.40
3	0.8663	3.75
4	0.8482	4.55

layers leads to a decrease in model performance and an increase in computation time. As the number of layers grows, the correlation coefficient (R) decreases and the MSE rises. This phenomenon can be attributed to the increasing complexity of the model, which, as it becomes excessively specialized in memorizing the training data, fails to generalize effectively to new data. This results a decrease R and an increase in MSE.

Consequently, the most compelling modeling results, characterized by favorable convergence and optimal model performance, are observed when using a single hidden layer. These results are in line with those of El Badaoui and colleagues [25]. In the interest of identifying the optimal model, the present study will be limited to a single hidden layer.

In order to identify the optimum number of neurons in the hidden layer, a study was conducted in which the number was varied from 1 to 20. The most effective characteristics for database distribution and the number of hidden layers were utilized. The figure below illustrates the variations in the MSE and the correlation coefficient (R) for different numbers of neurons in the hidden layer.

The results indicate that the MLP model has the highest correlation coefficient and the lowest mean square error when there are fifteen neurons in the hidden layer, compared to those for other hidden neuron numbers, ranging between 1 and

20. This configuration is characterized by an optimal balance between model complexity and accuracy. The finding suggests that a reduction in the number of neurons may result in underfitting, which could potentially lead to suboptimal outcomes. Conversely, an excess of neurons can lead to overfitting, resulting in unnecessary complexity without significant performance enhancements. This phenomenon, known as the overfitting problem, is well-documented in the field of neural network optimization, as demonstrated in the Figure 4 that increasing the number of neurons beyond a certain point does not necessarily improve performance and may even worsen it due to overfitting and increasing computational complexity[26].

A decision operator is defined as the activation function that evaluates the neuron's output condition based on its potential [27].
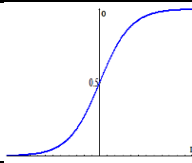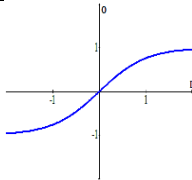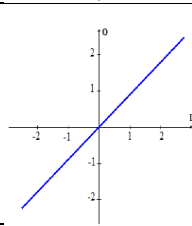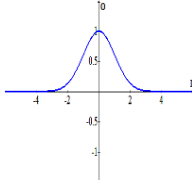
Various activation functions limit the amplitude of the neuron's output signal, thereby enabling the replication of the threshold effect observed in neurons. The main transfer functions that can be used as the neuron's activation function are shown in Table 3.

The sigmoid activation function is notable in that it facilitates the network capacity to handle both pure linear and non-linear problems. Considering this, we conducted a comprehensive investigation, assessing all possible combinations of activation functions in both the hidden and output layers. As demonstrated in the Table 4 below, the combination of activation functions (Tansig and Purelin) yielded the most favorable statistical results, with a correlation coefficient value of 0.9782 and a mean squared error of $1.58 \times 10^{+2}$. In this study, four distinct learning algorithms were utilized. Each of them is used in a specific way because of its high performance:
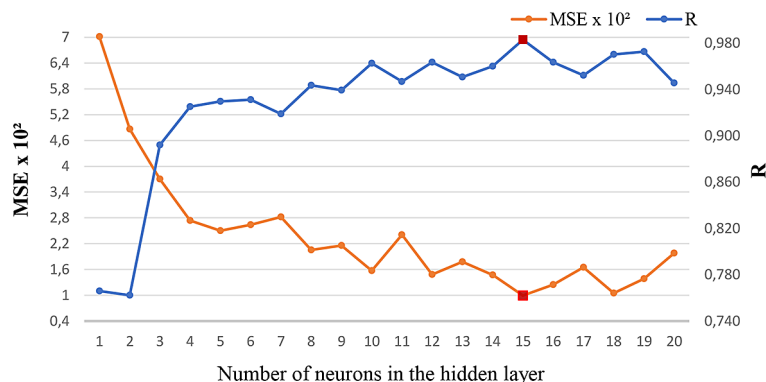
Figure 4. Values of the performance indicators R and MSE as a function of the number of neurons in the hidden layer

Table 3. Most commonly used activation functions in neural networks: formulas and graphs

Activation function	Formulas	Graphs	Application
Sigmoid	$f(x) = Logsig(x) = \frac{1}{1+\exp(-X)}$ Output range: (0,1)		Classification, regression
Hyperbolic tangent	$f(x) = Tansig(x) = \frac{2}{1+\exp(-2X)} - 1$ Output range: (-1,1)		Classification, regression
Pure linear function	$f(x) = Purelin(x) = x$ range: $(-\infty, +\infty)$		Output layers in regression problems
Gaussian	$f(x) = \exp\left(-\frac{x^2}{2}\right)$		Radial basis function networks Modeling, clustring

Table 4. Mean square errors and correlation coefficients in the learning phase for different combinations of activation functions

Hidden layers	Output layers	Designation	R	MSE x 10^{+2}
Tansig	Tansig	TT	0.9621	1.76
Tansig	Logsig	TL	0.8512	8.57
Tansig	Purelin	TP	0.9782	1.58
Logsig	Logsig	LL	0.7967	10.97
Logsig	Tansig	LT	0.9139	2.68
Logsig	Purelin	LP	0.9109	4.19
Purelin	Purelin	PP	0.9020	2.96
Purelin	Logsig	PL	0.8864	7.89
Purelin	Tansig	PT	0.9254	2.17

- gradient descent back propagation (GD),
- scaled conjugate gradient (SCG),
- resilient back propagation (RBP),
- Levenberg-Marquardt (LM).

The performance of each learning algorithm was assessed by considering the MSE, correlation coefficient (R), and the number of iterations.

As demonstrated in the following table, the Levenberg-Marquardt algorithm exhibits superior performance in terms of convergence speed and the statistical indicators R and MSE. This can be attributed to the fact that the algorithm rapidly converges towards the minimum squared error value, that it is highly processing efficient, and that it is suitable for meteorological prediction. The method is based on iterative gradient descent of the quasi-Newton family, incorporating non-linear least-squares methodologies, and the Gauss-Newton algorithm with constrained neighborhoods [28].

Table 5 provides a summary of the examined learning algorithms including their designations,

Table 5. Mean square errors and correlation coefficients in the learning phase for different learning algorithms

Learning algorithms	Designation	R	MSE x 10^{+2}	Iterations
Gradient descent (GD)	Traingd	0.8718	8.02	1000
Scaled conjugate gradient (SCG)	Trainscg	0.9747	1.25	287
Baysian regulation (BR)	Trainbr	0.9606	1.04	5
Levenberg-Marquardt (LM)	Trainlm	0.9809	0.99	4

the values of the R and MSE statistical indicators, and the number of iterations.

The optimal MLP model developed for predicting relative humidity in the city of Fez uses the pair of activation functions (Tansig-Purelin) and the Levenberg-Marquardt learning algorithm. The configuration of this model is [7-15-1], as illustrated in Figure 5.

The model comprises seven neurons in the input layer for the independent variables, fifteen neurons in the hidden layer, and one neuron in the output layer for the dependent variable (relative humidity).

RBF neural network

The RBF artificial neural network consists of an input layer with seven neurons and an output layer. The input layer neurons are activated by the following inputs: Temperature at 2 m, shortwave radiation, diffuse shortwave radiation, precipitation total, evapotranspiration, vapor pressure deficit and wind speed. The hidden layer neurons are activated by a gaussian function, while the output layer neuron is activated by a linear function (Table 6).

The RBF network demonstrated optimal performance when the gaussian function was used in the hidden layer and the linear function in the output layer, utilizing a [7-16-1] architecture. This configuration resulted in the highest correlation coefficient (R = 0.9603) and the lowest mean square error, demonstrating its superior predictive capacity (Fig. 6).
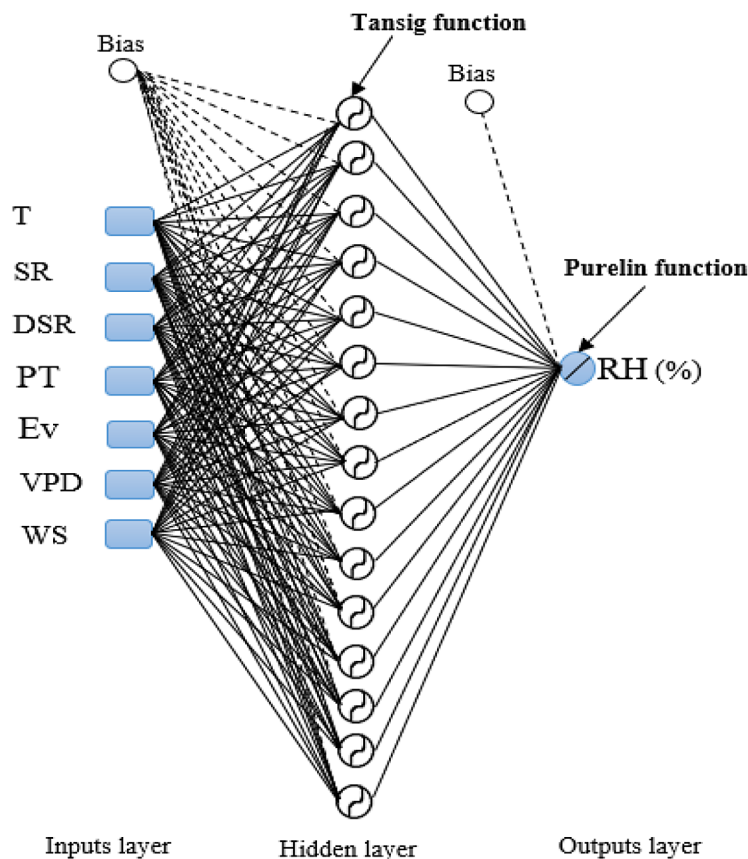
Figure 5. Architecture of the multilayer perceptron neural network developed in this configuration study [7-15-1]

Table 6. Performance of the RBF neural network model as a function of the number of neurons in the hidden layer

Number of neurons in the hidden layer	R	MSE × 10^{+2}
1	0.8242	6.36
2	0.9070	3.44
3	0.8561	4.51
4	0.9000	3.50
5	0.9113	3.21
6	0.9341	2.50
7	0.9157	3.27
8	0.9360	2.24
9	0.9352	2.39
10	0.9500	1.85
11	0.9492	1.79
12	0.9441	2.29
13	0.9463	2.30
14	0.9413	2.34
15	0.9603	1.50
16	0.9603	1.41
17	0.9552	1.69
18	0.9467	1.91
19	0.9525	1.86
20	0.9582	1.63

Comparison of the models developed

This study has produced several models that will be compared to determine the most suitable and effective model for predicting the relative humidity of the city of Fez (Morocco). The models include the classical MLR model, as well as the MLP and RBF artificial neural network models. We will compare the performance indicators (R and MSE) of these models to ascertain which one performs best.

According to the values of R and MSE statistical indicators (Table 7), the MLP model using artificial neural networks outperforms the model obtained by MLR. The MLP model performs better in all three phases: learning, validation, and testing, and maintains consistent performance across all three phases compared to the MLR-based model.

The Table 7 results demonstrate that both the MLP and RBF artificial neural network models are effective in the learning, validation, and testing phases. The predictive models developed by these networks show a strong correlation between the estimated and observed values, as indicated by the close correlation
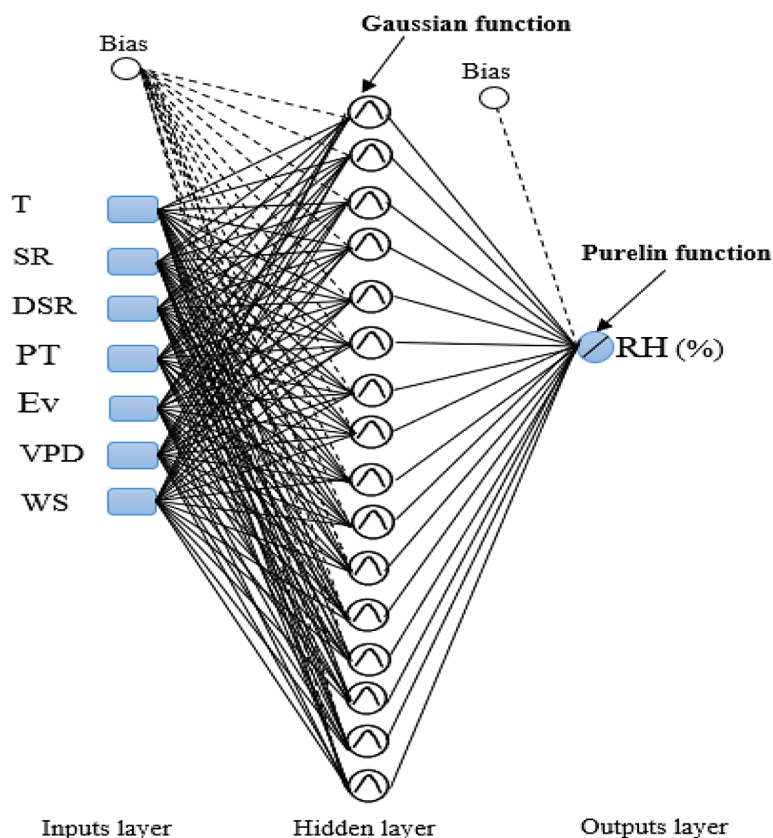

Figure 6. Architecture of the radial basis function neural network developed in this configuration study [7-16-1]

Table 7. Statistical indicator values for the two models MLR and ANN (MLP and RBF)

Model	R			MSE		
	Training	Validation	Test	Learning	Validation	Test
MLR	0.9023	0.8882	0.8882	58.0803	63.3014	63.3014
MLP	0.9809	0.9813	0.9813	0.0099	0.0097	0.0097
RBF	0.9603	0.9607	0.9607	0.0141	0.0140	0.0140
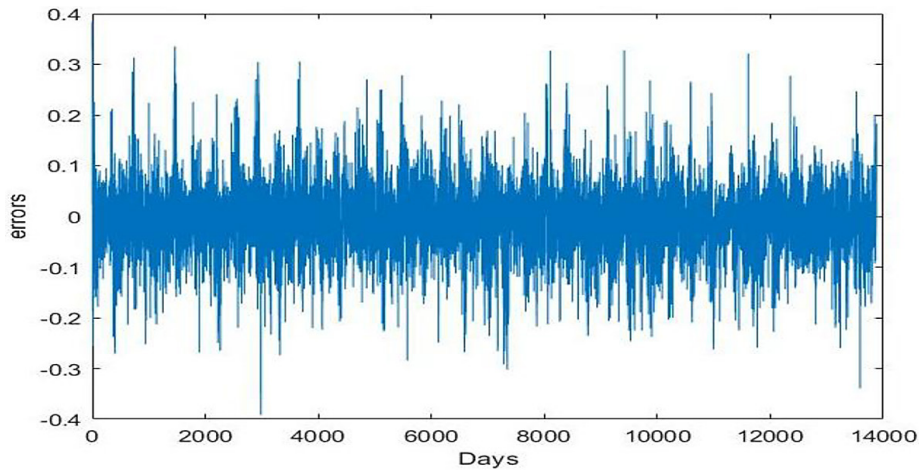
Figure 7. Difference between real and predicted values of relative humidity using an MLP model in forecasting
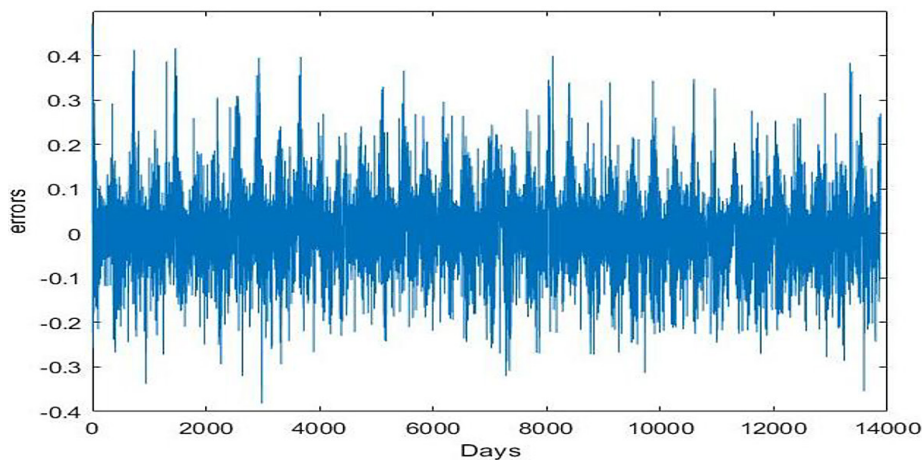
Figure 8. Difference between real and predicted values of relative humidity using an RBF model in forecasting

coefficients obtained for all three phases. This highlights the advantage of using these ANN models for predicting relative humidity in Fez. Additionally, the MLP network's learning phase is faster than that of the RBF network, converging rapidly with a smaller number of iterations.

The difference between the predicted and measured values for the RBF model is less than 0.3 (Figure 7), while for the MLP model, it is less than 0.2 (Figure 8). This suggests that the MLP is more resilient than the RBF model

The developed MLP model exhibits a high degree of accuracy, with the majority of predictions demonstrating an error margin of less than 0.2. This finding indicates that, in the majority of cases, the observed and predicted values are similar, suggesting an optimal prediction for this data set.

CONCLUSIONS

It is crucial to develop a mathematical model using artificial neural networks to predict relative humidity in aquatic environments. Accurate relative humidity forecasts, updated by this model are vital for water resource management and conservation. Predicting changes in humidity enables better management of water reservoirs, maximizes agricultural irrigation and protects aquatic ecosystems from severe weather events such as floods and droughts. In conclusion, the ANN to the modeling of relative humidity is a major step toward the effective and sustainable management of water resources, benefiting both the environment and the populations who depend on these resources.

To this end we developed black box models to predict the relative humidity in the city of Fez using MLP and RBF artificial neural networks.

In our case study, we created several mathematical models, including the classical MLR model, as well as the MLP and RBF artificial neural network models. To assess their predictive performance, we examined their architectures, learning algorithms, correlation coefficients, and mean square errors. The comparison between the two MLR models and the MLP neural networks showed that the relative humidity of the city of Fez is related to the other meteorological parameters by a non-linear relationship. This work verified the ability of neural networks for learning and prediction in the meteorological domain.

The study concluded that MLP models are generally more flexible and adaptable to a variety of problems. They can approximate functions of different shapes, unlike RBF networks. The findings of the present study indicate that the Architectural MLP [7-15-1] is the most suitable model for predicting relative humidity. This model employs the pair activation functions (Tansig-Purelin) and the Levenberg-Marquardt algorithm, yielding a correlation coefficient of 0.9809 and a reduced mean square error of 0.0099.

Acknowledgement

REFERENCES

1. Xie B., Zhang Q., and Ying Y. Trends in precipitable water and relative humidity in China: 1979–2005. Journal of Applied Meteorology and Climatology. 2011; 50(10): 1985–1994. https://doi.org/10.1175/2011JAMC2446.1

2. Lowen A. C., Mubareka S., Steel J., and Palese P. Influenza virus transmission is dependent on relative humidity and temperature. PLoS Pathogens. 2007; 3(10): 1470–1476. https://doi.org/10.1371/journal.ppat.0030151

3. Park J.-E., Son W.-S., Ryu Y., Choi S. B., Kwon O., and Ahn I. Effects of temperature, humidity, and diurnal temperature range on influenza incidence in a temperate region. Influenza and Other Respiratory Viruses. 2020; 14 (1): 11–18. https://doi.org/10.1111/irv.12682

4. Ma Y. et al. Effects of temperature variation and humidity on the death of COVID-19 in Wuhan, China. The Science of the Total Environment, 2020; 724: 138226. https://doi.org/10.1016/j.scitotenv.2020.138226

5. Mecenas P., Bastos R. T. da R. M., Vallinoto A. C. R., and Normando D. Effects of temperature and humidity on the spread of COVID-19: A systematic review. PloS One. 2020; 15(9): e0238339. https://doi.org/10.1371/journal.pone.0238339

6. Bennedsen M. Designing a statistical procedure for monitoring global carbon dioxide emissions. Climatic Change. 2021; 166(3): 32. https://doi.org/10.1007/s10584-021-03123-y

7. Sisco M. R., Bosetti V., and Weber E. U. When do extreme weather events generate attention to climate change Climatic Change. 2017; 143(1): 227–241. https://doi.org/10.1007/s10584-017-1984-2

8. Kuzugudenli E. Relative humidity modeling with artificial neural networks. Applied Ecology Environmental Research. 2018; 16(4): 5227–5235. https://doi.org/10.15666/aeer/1604_52275235

9. Liaw A. and Wiener M. Classification and regression by random forest. R News. 2007; 2(3): 18–22.

10. Hanoon M. S. et al. Developing machine learning algorithms for meteorological temperature and humidity forecasting at Terengganu state in Malaysia. Scientific Reports. 2021; 11(1): 18935. https://doi.org/10.1038/s41598-021-96872-w

11. Yahia B. A., Abdallaoui A., and Kadir I. Development of a stochastic model of RBF neural network for forecasting relative humidity rates. International Conference on Circuit, Systems and Communication (ICCSC). 2024; 1–7. https://doi.org/10.1109/iccsc62074.2024.10617431

12. Khatibi R., Naghipour L., Ghorbani M. A., and Aalami M. T. Predictability of relative humidity by two artificial intelligence techniques using noisy data

from two Californian gauging stations Neural Computing and Applications. 2013; 23(7): 2241–2252. https://doi.org/10.1007/s00521-012-1175-z

13. El Badaoui H., Abdallaoui A., & Chabaa S. Using MLP neural networks for predicting global solar radiation. The International Journal of Engineering and Science (IJES). 2013; 2: 48–56.

14. Touzet C. Artificial neural networks, introduction to connectionism. EC2 (in Frenche). https://doi.org/10/document

15. Heidari E., Sobati M. A., and Movahedirad S. Accurate prediction of nanofluid viscosity using a multilayer perceptron artificial neural network (MLP-ANN). Chemometrics and Intelligent Laboratory Systems. 2016; 155: 73–85. https://doi.org/10.1016/j.chemolab.2016.03.031

16. Derras B., Bekkouche A., and Zendagui D. Neuronal Approach and the Use of KIK-NET N Response Spectrum on the Surfaceetwork to Generate. Jordan Journal of Civil Engineering. 2010; 4(1).

17. Manssouri I., Manssouri M., and Kihel B. Fault detection by K-NN algorithm and MLP neural networks in a distillation column: Comparative study. Knowledge Management and Communication in the Information. 2013 ; 201–215.

18. Bélanger M., El-Jabi N., Caissie D., Ashkar F., and Ribi J. Estimation de la température de l'eau de rivière en utilisant les réseaux de neurones et la régression linéaire multiple. Revue Science de l'eau/Journal of Water Science. 2005 18(3) : 403–421. https://doi.org/ 10.7202/705565ar

19. Ghorbani M. A., Zadeh H. A., Isazadeh M., and Terzi O. A comparative study of artificial neural network (MLP, RBF) and support vector machine models for river flow prediction. Environmental Earth Sciences. 2016; 75(6): 476. https://doi.org/10.1007/s12665-015-5096-x

20. Broomhead D. S. and Lowe D. Multivariable functional interpolation and adaptive networks. Complex Syst. 1988; 2(3).

21. Moody J. and Darken C. J. Fast learning in networks of locally-tuned processing units neural computation. 1989; 1(2): 281–294. https://doi.org/10.1162/neco.1989.1.2.281

22. Boudebbouz B., Manssouri I. Mouchtachi A., Manssouri T., and Kihel B. E., Use of RBF artificial neural networks to model the normal regime with variable operating point of an industrial plant. European Scientific Journal, ESJ. 2015; 11(18) (in French).

23. Chen K. T., Chou C. H., Chang S. H., and Liu Y. H. Intelligent active vibration control in an isolation platform. Applied Acoustics. 2008; 69(11): 1063–1084. https://doi.org/10.1016/j.apacoust.2007.06.008

24. El Azhari K., Abdallaoui B., Dehbi A., Abdallaoui A., and Zineddine H. Development of a neural statistical model for the relative humidity levels prediction in the Region of Rabat-Kenitra (Morocco) Research Square. 2021. https://doi.org/10.21203/rs.3.rs-385467/v1

25. El Badaoui H., Abdallaoui A., & Chabaa S. Multilayer Perceptron and Radial Basis Function network to predict the moisture. International Journal of Innovation and Scientific Research. 2014; 5(1).

26. Hinton G. E. and Salakhutdinov R. R. Reducing the dimensionality of data with neural networks. Science. 2006; 313 (5786): 504–507. https://doi.org/10.1126/science.1127647

27. El Badaoui H., Abdallaoui A., & Chabaa S. Optimization numerical the neural architectures by performance indicator with LM learning algorithms. Journal of Materials and Environmental Science. 2017; 8: 169–179.

28. Wilamowski B. M., Iplikci S., Kaynak O., and Efe M. O. An algorithm for fast convergence in training neural networks. International Joint Conference on Neural Networks (IJCNN'01). 2001; 3: 1778–1782. https://doi.org/10.1109/ijcnn.2001.938431